Structural, electronic, magnetic, and transport properties of carbon-fullerene-based polymers

Chapter · February 2010

DOI: 10.1093/oxfordhb/9780199533053.013.21

4 authors:

Antonis Andriotis
Foundation for Research and Technology - Hellas
158 PUBLICATIONS **3,943** CITATIONS
SEE PROFILE

R. Michael Sheetz
University of Kentucky
26 PUBLICATIONS **651** CITATIONS
SEE PROFILE

Ernst Richter
University of Kentucky
61 PUBLICATIONS **3,725** CITATIONS
SEE PROFILE

Madhu Menon
University of Kentucky
244 PUBLICATIONS **8,373** CITATIONS
SEE PROFILE

Structural, electronic, magnetic, and transport properties of carbon-fullerene-based polymers

21

A. N. Andriotis, R. M. Sheetz, E. Richter, and M. Menon

21.1 Introduction

The origin of magnetism in carbon-based (C-based) materials can be unambiguously attributed to the presence of defects, namely carbon vacancies (C_vs), edge states, other structural and/or topological defects and non-magnetic impurity atoms (IAs) (Andriotis *et al*. 2003, Lehtinen *et al*. 2004). The role of defects appears to be dual; i.e. they may participate in the formation of the magnetic moments and may mediate their magnetic coupling by developing the proper interaction pathways. The magnetic moments are usually provided by the defect sites themselves and their surrounding sites that act as sites of spin localization. Thus, we can define a magnetic unit cell (MUC) associated with each defect and its surrounding atoms that is associated with a magnetic moment. The appearance of macroscopic magnetism is then associated with the magnetic coupling of these MUCs.

In a series of reports(Andriotis *et al*. 2003, Andriotis and Menon 2005, Andriotis *et al*. 2005a, 2005b, 2007, 2006a), we have shown that in the C_{60}-based polymers, the magnetic interaction pathway may be attributed to the fields of large electric dipole moments resulting from charge transfer among two types of defects, namely the C_vs and the $2+2$ cycloaddition bonds, which act as donor (D) and acceptor (A) sites, respectively. On the one hand, the presence of D- and A-sites makes the electron-charge distribution take the form of a charge-density wave (CDW)-like disturbance. We, then, observed that if the C_v is considered as a donor unit and the $2+2$ cycloaddition bond as an acceptor unit in the sense of McConnell's approach to magnetism of charge-transfer salts (McConnell and Welch 1967), then the magnetism of the

C_{60}-based polymers could be explained in terms of a generalized McConnell model (Andriotis *et al*. 2005a, 2005b). In such an approach, the stabilization of the magnetic state is attributed to the kinetic exchange (McConnell and Welch 1967) interaction, i.e. a configuration interaction (CI) effect; (see Section 21.5.1). On the other hand, the spin-density localizations make the spin-density appear as a spin-density wave (SDW)-like disturbance reminiscent of the layered magnetic materials (Baibich *et al*. 1988, Samant *et al*. 1994).

Both the CDW- and the SDW-like disturbances in the electron charge and spin densities and their possible relationship to the carbon magnetism (Andriotis *et al*. 2003, Andriotis and Menon 2005, Andriotis *et al*. 2005a, 2005b, Andriotis 2007, 2006a) motivated us to investigate whether the C_vs can be simulated by some impurity atoms. In other words, we wondered whether the action of a C_v can be replaced by a similar action of an impurity atom such as boron that is more electropositive than carbon. With this objective in mind, we performed a series of calculations on the C_{60}-based polymer and a single-walled carbon nanotube (SWCN), either without defects or with C_vs and/or non-magnetic IAs, namely N, B, P, O and S (Andriotis *et al*. 2006b), with varying degrees of electronegativities (some more and some less) relative to carbon. As will be discussed in the following, none of the investigated substitutional impurities can simulate the role of the C_v in the development of magnetism in the C_{60}-based polymer.

Further investigations of the defect-induced magnetism led us to identify similarities between the magnetic features of the C_{60}-based polymers and those of some non-traditional inorganic materials (NTIMs), the latter including oxides like ZnO, TiO_2, CaO, HfO_2, ZrO_2, etc., as well as other members of the wide class of the diluted magnetic semiconductors (DMSs) (Andriotis and Menon 2005, Andriotis *et al*. 2005a, 2005b, 2007, 2006a). A cursory look does not reveal any (at least strong) correlation between, say, the carbon magnetism and that of the D-NTIMs materials. For example, in the NTIMs doped with 3*d* magnetic impurities, the spin-resolved *d*-band, which plays a dominant role in the development of magnetism, has no analog in the C-based materials. However, a careful look and an indepth analysis of the reported results reveal a strong correlation among them with identifiable common features (Andriotis and Menon 2005, Andriotis *et al*. 2005a, 2005b, 2007, 2006a). In particular, our recent study has led us to the conclusion that these two classes of magnetic materials share several common features that include:

- point defects (structural, topological, vacancies, substitutional and/or interstitial impurities);
- physical processes that appear as the consequence of the existence of the defects, i.e. charge and spin transfer and localization, rehybridization of electron states, frustration, states in the gap, degenerate or resonant ground state driven by electron–electron correlations, etc.;
- common ferromagnetic coupling pathways among the unpaired electrons as, for example, the proposed hydrogen-mediated coupling pathway (Chan *et al*. 2004, Park and Chadi 2005);

- enhanced ferromagnetic features when codoped, i.e. in the simultaneous presence of two different dopants, or equivalently, in the simultaneous presence of two kinds of defects (of structural/topological or of substitutional-impurity type) (Andriotis *et al*. 2007).

In simple metals doped with magnetic impurities, the magnetic moments associated with the defects are provided by the magnetic IAs, i.e. they are of *extrinsic* character in contradistinction to the *intrinsic* character of those of the C-based materials; the magnetic coupling among them depends on the strength of the interaction between the magnetic moment of the IA and the spin of the carrier (electron). This interaction acting as a perturbation on the carrier wave-functions becomes responsible for the magnetic coupling, the latter known as the Ruderman–Kittel–Kasuya–Yosida (RKKY) interaction (Ruderman and Kittel 1954, Kasuya 1956, Yosida 1957). This picture is generalized in the case of the DMSs where electron holes may also appear as the charge carriers. In the latter case, the magnetic coupling may be attributed to the formation and the mutual interaction of bound magnetic polarons (Dietl 2006, Kuroda *et al*. 2007).

Contrary to the case of systems including magnetic IAs, in magnetic carbon materials and in some of NTIMs, in which the magnetic moments are of intrinsic type, i.e. they are induced and therefore provided by the defects, the description of the magnetic state is more complicated; it depends strongly on the response of the system to the presence of the defects. In particular, the response of the atoms neighboring the defects appears to be crucial. This is mainly expressed in the form of charge transfer from or towards the defect sites. Factors such as the point-group symmetry of the defect sites, the type of the defects, the band-filling and band-splitting factors of the atomic orbitals of the IA and the neighboring defect atoms are all very important (Mpourmpakis *et al*. 2003, 2005). However, the ferromagnetic coupling among neighboring magnetic moments is not only a local effect leading to the formation of a magnetic moment, it depends crucially on the mutual interaction between the magnetic moments that is established by the induced charge transfers. This is a complicated interaction that, as Sinha and Ramasesha (1993) have shown, depends on the inter- and intrasite Coulomb interactions (Sinha and Ramasesha 1993). That is, it depends strongly on the electron–electron *e–e* correlations.

Despite the intense theoretical and experimental investigations, the origin of the magnetism of the C-based materials (as well as that of the D-NTIMs) is not well understood so far, owing perhaps due to the limitations of both theory and experiment. Nevertheless, it is well understood that magnetism is a result of *e–e* correlations and as such it is well understood that the *s–p* magnetism is also a manifestation of the *e–e* correlation effects and, therefore, the magnetism of these materials has a common origin, that of the *e–e* correlations, as extensively discussed by us (Andriotis *et al*. 2005a). Although this is well understood, a clear picture of the way these correlations contribute to magnetism is missing so far. In other words, it is not well understood what are the fundamental electronic processes that give the most pronounced contributions to magnetism and what is the physical reasoning for this behavior. Such knowledge is of

fundamental interest not only from the academic point of view but also for the technology because the latter relies on this information in order to develop those pathways that can lead to efficient tailoring of the magnetic features of these materials.

Our limited understanding of the magnetism of the C-based materials and the D-NTIMs stems on the one hand, from the inadequacy of the popular single reference DFT/GGA computational tools to incorporate *e–e* correlations in a satisfactory and efficient way and, on the other hand, from the fact that computational tools that can go beyond the DFT/GGA (as, for example, CI-levels of approximation) are computationally prohibitive.

In the present work we discuss the defect-induced ferromagnetism of the C_{60}-based polymers and its analog in the case of NTIMs. In Section 21.2, we review the computational methods that are currently in use in the literature and point out the pros and cons of each one of them and describe the methods we use. In Section 21.3, we describe the defects associated with the ferromagnetism of the C_{60}-based polymers, namely the C_vs, the $2 + 2$ cycloaddition bonds and impurity atoms, and demonstrate their effect on the electronic structure. The effect of codoping is also discussed. In Section 21.4, we investigate in detail the electronic, magnetic and transport properties of the rhombohedral C_{60}-polymer. In Section 21.5, we discuss the origin of magnetic coupling among the magnetic moments in the rhombohedral C_{60}-polymer and propose a generalization of McConnell's model for its justification. We also provide further evidence for the analogy between the magnetism of the rhombohedral C_{60}-polymer and the ZnO, the latter codoped with Co^{2+} and Cu^{+} ions. Finally, in Section 21.6, we summarize our conclusions.

21.2 Computational methods

Reviewing the theories and the computational methods that were proposed to explain the magnetism of the above-mentioned materials, it can be seen that they may be thought of as belonging to two major classes. The first includes single reference models (SRMs), i.e. theories that use one Slater determinant to describe the electronic structure of the ground state. The second uses a multireference approach and we refer to this class as configuration interaction (CI) models (CIMs). For both classes, the objective appears to be the incorporation of the electron-correlation effects in the Hamiltonian of the system in an efficient and computationally tractable way.

The CIMs include various computational schemes as, for example, van Vleck's approach to the magnetism of bulk Ni (van Vleck 1953), Ovchinnikov's spin-polarization model (Ovchinnikov 1978, Ovchinnikov and Shamovsky 1991), McConnell's model (McConnell and Welch 1967), the superexchange model of Zener–Anderson–Hasegawa (Zener 1951a, Zener 1951b, Anderson and Hasegawa 1955), etc. As some of these approaches are applicable to the ordinary magnetism of the 3*d* metals, one can trace the electron-correlation effects to be the common origin of both the magnetism of the 3*d* metals and that of the d^0-type, the latter term assigned to the *s–p* magnetism appearing in the absence of *d*- or *f*-electrons, i.e. of those unpaired

electron states that are usually responsible for the occurrence of magnetic phenomena (Andriotis *et al*. 2005a, 2005b, 2007, 2006a).

21.2.1 Single versus multireference descriptions

The successful application of any of the CIMs depends on their ability to identify those electronic configurations responsible for the major contribution to the correlation energy. This automatically calls for attention to the known computational *state specific approaches* that were used in computational chemistry and were proposed for treating the correlation energy (see, for example, Nicolaides *et al*. 1984 and references therein). It is worth noting that within the CIMs, the system may be *simultaneously* in various electronic configurations. This may be translated by saying the electron may spend some of its time in each one of these configurations. Thus, in this view, one can consider the CIMs as giving a description of a *dynamic* picture of the system, that is, a picture of the system whose state is r*esonating* among a few of its low-lying configurations.

On the other hand, in the SRMs, the electron correlation is usually incorporated as an average effect, i.e. as a spatial term affecting the Hamiltonian of the system. In this view, the SRMs describe an average *static* picture that is justified by previously obtained *ab-initio* theoretical results. The SRMs may be used for the development of semi-empirical approaches whose successes depend on their simplicity and their effectiveness in describing the major part of the correlation effects by an additional (frequently assumed perturbational) spatial Hamiltonian term (Bouzerar and Ziman 2006).

Whether a static (SRM) or a dynamic (CIM) description is more appropriate or not, this depends on the system under investigation. For example, when the defect creates more than one topologically equivalent electronic configurations then, a CIM description seems to be more appropriate. By contrast, SRM methods seem appropriate when structural topological degeneracy is absent. The latter appears to be the case of a C_v in a finite nanographeme layer where, due to relaxation, the sites around the vacant site are not all exactly equivalent. A similar situation appears in the oxygen sites around a Zn-vacancy in a finite ZnO nanocrystal. In such cases as in these examples, the LDA/GGA approximation level of the DFT theory may be successfully used in *ab-initio* simulations.

Thus, although the exchange coupling among lone-electron spins could be attributed to the CI (McConnell and Welch 1967, Sinha and Ramasesha 1993, Ovchinnikov 1978, Shibayama *et al*. 2000), however, the success of the DFT/GGA or that of a hybrid DFT approach within the GGA (to be denoted as hDFT/GGA[1]), in describing the magnetic features of the Rh-C_{60} reveals the existing possibility of mapping the *dynamical* picture of the CI theory onto the *static* picture of the (h)DFT/GGA method (Andriotis *et al*. 2003, Lehtinen *et al*. 2004). This means that spin-resolved (h)DFT/GGA could, in principle, describe well the electron delocalization and the associated charge and spin-density accumulations induced by the defects. This is attributed to the feature of the (h)DFT/GGA to address partially filled molecular orbitals (MOs) and one of the advantages in using the (h)DFT/GGA is that it allows us to give a

Q2

[1] In the following, the symbol (h)DFT will be used to indicate any of DFT/LDA, DFT/GGA or hDFT/GGA unless specified otherwise.

description of the magnetic state in terms of the overlap of MOs associated with the lone-electron spins.

The CI approach has the unique ability of being able to describe an electron in *resonance* among various close-lying MOs. The question that still remains is to what extent the CI approach can be replaced by that of a SR-DFT scheme. Equivalently, the question is: which one of the two schemes (the CI or the SR-DFT scheme) can incorporate efficiently the effect of the electron–electron correlations for magnetic systems in computer simulations.

Technically speaking, this is more or less equivalent to the question about the capability of the SR-DFT schemes to describe satisfactorily the spin-density localization and the electron delocalization, both of which become pronounced in nanosystems. This, in turn, is related to the efficiency of the system to locally screen the perturbations caused by its own defects. The effective screening that is developed in bulk and, especially, conducting materials is significantly reduced in nanosystems resulting in the latter developing remote delocalization of charge and spin density due to point defects. This is contrary to the case of the bulk jellium or periodic-lattice metal in which these perturbations appear locally and decay in the form of Friedel oscillations as they get away from the perturbing defect.

21.2.2 Adequacy of single-reference approaches

The local character of the DFT/GGA and the fact that electron delocalization depends on the intersite transfer integral and the strength of the on-site Coulomb correlations (Sinha and Ramasesha 1993) cannot guarantee a priori a possible success of a DFT/GGA scheme. One can add to these drawbacks the inadequacy of the DFT/GGA to address excited states in a satisfactory way, making it inappropriate for describing the low-lying spin states. The adequacy of the DFT-based schemes could be enhanced if schemes beyond the DFT/GGA (as, for example, time-dependent perturbation theory, suitable SIC/DFT combined with the DFT/GGA+U, etc.) are used. It appears that a successful application of a hDFT/GGA scheme becomes *system specific* as this depends on other criteria as well, as for example, how well the method reproduces the bandgap, the spin-polarization, the relative position of majority and minority impurity spin states relative to the energy gap, etc.

Generalizing previous observations (Fink 2006), it can be claimed that DFT calculations can only be used if the ground state of the system (and, therefore, of each MUC) is spatially non-degenerate and the chosen exchange and correlation function used is adequate. For spatially degenerate MUC states, it is well known that the dynamic picture of the CI description cannot be mapped satisfactorily onto the static DFT one. Therefore, the superexchange coupling between two MUCs can no longer be described by a simple Lande splitting (Fink 2006).

Focusing on the magnetism induced by carbon vacancies in the C_{60}-based polymers (Andriotis *et al*. 2003), it is observed that the spin density surrounding the vacant sites in a C_{60}-dimer (having one C_v per C_{60} molecule) is not uniformly distributed in either one of the two MUCs (i.e. the two C_{60} molecules)

or among the three C-atoms neighboring each vacant site. This means that a DFT description could have been expected to be a good approximation for the description of this MUC (although the charge and spin density obtained with the hDFT/GGA scheme may not correctly reflect the degeneracies of the MUC). A different situation is encountered in the CI description of the double-exchange interaction in Mn−O−Mn radicals proposed by Anderson and Hasegawa (Anderson and Hasegawa 1955) in which a CI approach appears more effective. Furthermore, the coupling among the magnetic moments of neighboring MUCs depends on their mutual interaction that is established by the induced charge transfers. This is a complicated interaction that depends strongly on Coulombic electron correlations. It should, therefore, be understood that the success of a (h)DFT/GGA to describe the inter-MUC interaction in systems with induced magnetic moments depends on its ability to describe accurately:

- the charge transfer induced by the defects;
- the magnetic state of the individual MUCs; and
- the magnetic coupling among the magnetic moments of the MUCs.

21.2.3 Model approximations

One can exploit the local character of the DFT/GGA scheme and introduce some empirical extensions to it in an attempt to simulate the correct CI results. For example, the charge accumulation around a Zn vacancy in ZnO was approximated by adding an on-site potential term on the oxygen sites surrounding the vacancy (Bouzerar and Ziman 2006). Such empirical approximations are helpful in investigating the ferromagnetic coupling (FMC) among the defect-induced magnetic moments by mapping the empirically obtained exchange interactions onto the Heisenberg model. However, they do not give a thorough view of the induced magnetism and their use may not adequately address the consistency issue described by the criteria set in (Osorio-Guillen *et al*. 2006).

21.2.4 Brief review of the methods used in the present work

Our present work investigates the effect of the defects in C_{60}-based polymers and, in parallel, in the SWCNs; it belongs to the class of the SRMs and utilizes *ab-initio* computational methods. Our computational approach is justified from the fact that in nanoparticles of both the C_{60}-based polymers and the SWCNs, the defects do not lead to structurally degenerate ground states.

All our structures are fully relaxed. Small clusters are investigated using the Gaussian-03 code (Gaussian 2003) within the B3LYP level of approximation to the exchange and correlation energy using the 6–311 G** basis set. The stability of our results was checked by including dynamic correlation effects using the UMPW1PW91 hybrid functional. **Q3**

Medium-size and larger clusters were investigated by employing the tight-binding molecular-dynamics (TBMD) method within a complete set of *s, p*

and *d* orbital functions at a level that has a firm *ab-initio* footing. Our TBMD scheme is the only scheme that allows full quantum MD relaxation of systems containing several hundred transition-metal atoms, while incorporating magnetic effects dynamically; it includes *e–e* correlation effects at the Hubbard-U approximation (Menon 1998, Andriotis and Menon 1998); it allows the incorporation of spin-orbit interaction (in the $\mathbf{L} \cdot \mathbf{S}$ approximation) and non-collinear magnetic effects (Andriotis and Menon 1998, 2004) as well as the effect of temperature (Fthenakis *et al*. 2003, Andriotis *et al*. 2006); it contains many unique features that make it ideally suited for the treatment of the materials problems of the present work. For large-scale simulations we have developed a parallel algorithm that enables molecular-dynamics simulations of systems containing atoms in excess of a thousand. This method is more accurate than the order-N methods that are being used at present to treat systems of these sizes. Our TB scheme has been applied with success in the case of C-based materials doped with TMs (see, for example, (Lathiotakis *et al*. 1996, Andriotis *et al*. 1998, 1999, 2000)). It has been proved to be ideal for studying structural and electronic properties of systems of the group-IV elements, their heterostructures as well as their interaction with transition metals (Andriotis and Menon 1998). Harrison's universal TB parameters are used, suitably parametrized with respect to the interatomic distance, in oder to describe the carbon–carbon interactions. For the carbon–Ni interactions, we use TB parameters reported in a previous publication (Andriotis *et al*. 1999).

Our TBMD formalism is used to calculate the electronic (band) structure and investigate the electronic transport properties by calculating their current–voltage (*I–V*) characteristics. We make use of the surface Green's function matching method (SGFMM) that employs the scheme that we proposed in our earlier reports (Andriotis and Menon 2001, Andriotis *et al*. 2002). In brief, the SGFMM (Andriotis and Menon 2001) is an embedding method. In this approach we followed Datta's formalism (Datta 1995) by incorporating it into Sanvito's *et al*. (1999) approach, with the latter suitably modified by implementing it according to the embedding approach of Inglesfield and Fisher (Andriotis 1992, 1990).

21.3 Defect-induced structural and electronic features

In the following, the term *defect* is ascribed to any type of point and/or structural and/or topological defects including vacancies (Hjort and Stafstrom 2000), edge states (Harigaya 2001, Harigaya and Enoki 2002), substitutional impurities (Matsumoto *et al*. 2001), Stone–Wales defects in graphite-based materials (Kim *et al*. 2003), orientational changes of structural units (as, for example, among the C_{60} molecules in the TDAE-C_{60}) (Narymbetov *et al*. 2000), adsorbed adatoms, (Lehtinen *et al*. 2003) etc. At present, a general consensus has been reached on the role of these defects in the development of magnetism in the graphitic and other carbon-based materials. According to this, most of these defects play more or less a common role in promoting a FM

ground state. That is, they break the sequence of the alternating single–double carbon bonds, inducing the response of the material in the form of charge and spin transfers that lead to the formation of lone electrons and their stable FM coupling.

In the present work, we will be focusing mainly on three of the above-listed defects, namely, the vacancies, the $2 + 2$ cycloaddition bonds and the impurity atoms.

21.3.1 Structural and topological defects; Vacancies and $2 + 2$ cycloaddition bonds

Polymerization of C_{60} leads to polymeric $2 + 2$ cycloaddition bonds, resulting in the development of significant lattice strains, the latter being proportional to the number of polymerization bonds developed. Polymeric C_{60} systems belong to the class of frustrated systems. Their basic characteristic is that they exhibit a huge number of configurations with the same energy and consequently have a distorted ground state with macroscopic degeneracy (Marques *et al*. 2003).

The vacancies can be created by removing one or more carbon atoms; they lead to under-coordinated C atoms. The experimental results on graphite vacancies have mainly been obtained from STM and TEM studies. It has been widely accepted that the symmetric (D_{3h}) vacancy is the most common monovacancy in graphite. However, recent reports claim that the asymmetric vacancy 5–1db (pentagon–one dangling bond) with (experimental) formation energy of 7.0 ± 0.5 eV has lower energy, while the symmetric vacancy is a result of a time-averaged superposition of three degenerate vacancy states alternating by a thermally activated Jahn–Teller effect (El-Barbary *et al*. 2003). It has also been found that the ground-state vacancy in graphite is spin free.

There are, however, contradicting reports concerning the charge state of the monovacancy. Hjort and Stafstrom (2000), using the Huckel approximation, found that the triad of the carbon atoms near a graphite vacancy move away from the vacancy site upon relaxation and each of these carbon atoms gets approximately 0.19 electrons originating from states near the Fermi energy (Hjort and Stafstrom 2000). This finding was claimed to be justified by STM measurements in which the vacancy is viewed as a bright spot (protrusion). Contradicting this is the work of Andriotis *et al*. (2003) that argued that in the case of a C_{60} dimer in which the two C_{60} molecules are bonded by a $2 + 2$ cycloaddition bond, the vacancy sites create a charge-density-wave-like (CDW-like) disturbance, with positive charge accumulation of approximately 0.5 electrons around the defect sites and an equal but opposite charge accumulation in the region of the $2 + 2$ cycloaddition bonds (see discussion below and Figs. 21.5 and 21.6). As a result, an electric dipole moment (EDM) of 2.264 Debye is developed (Andriotis *et al*. 2003).

The $2 + 2$ cycloaddition bonds are defects that break the alternating single and double bonds in the C_{60} polymers. Their formation requires neighboring C_{60} molecules to be oriented with their double bonds (Onoe and Takeuchi 1997). A full nearest-neighbor (nn) polymerized direction leads to an average

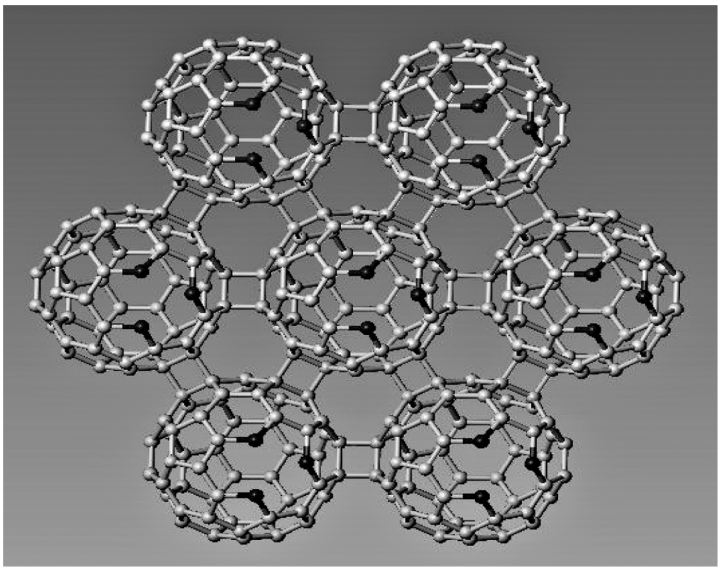

Fig. 21.1 Model structure for the rhombohedral C_{60} (Rh-C_{60}) polymer with one carbon vacancy (shown surrounded by carbon atoms highlighted in dark) per C_{60} molecule. The carbon atoms participating in the $2 + 2$ cycloaddition bonds form corners of the rectangles in the figure.

inter-C_{60} distance of 9.1–9.2 Å (while an unpolymerized nn distance is 10 Å at ambient pressure). This bond is known also as a 66/66 bond because it links two pairs of bonds with each one of the latter joining two hexagons in a C_{60} molecule. It may also happen that one or both bonds that are linked by the cycloaddition is a common bond between a hexagon and a pentagon. The resulting cycloaddition bonding then may be of the type 65/66 or 65/56, respectively. The relaxed 66/66, 65/56 and 65/66 bonds were found to have lengths 9.19, 9.17 and 9.26 Å, respectively (Okotrub *et al*. 2001). It is worth noting that C_{60} polymerization, i.e. the formation of the $2 + 2$ cycloaddition bonds, leads to a reduction and even to an elimination of the energy gap that is exhibited by the non-polymerized C_{60} solid. This tendency of the C_{60} polymers is enhanced if carbon vacancies are also present.

In Fig. 21.1, we show the model structure for the two-dimensional rhombohedral C_{60} (Rh-C_{60}) polymer with one C_v per C_{60} molecule. In this structure, each C_{60} molecule is bonded to six surrounding C_{60} molecules by $2 + 2$ cycloaddition bonds. Its electronic band structure and electron density of states (DOS) have been calculated using our TBMD formalism; they are shown in Figs. 21.2 and 21.3 for the defect-free and the defected case, respectively, the latter exhibiting one C_v per C_{60} molecule. From these, it is apparent that the presence of the C_vs eliminates the energy gap and, therefore, the imperfect Rh-C_{60} appears to be metallic. This supports the experimental evidence that the magnetism of the Rh-C_{60} polymer appears at the onset of the metal–insulator transition (Makarova *et al*. 2001, Makarova n.d.).

Q4

21.3.2 Substitutional impurities

In an attempt to simulate the C_v with an impurity atom, we have performed a series of calculations with a C_{60} dimer in which we replaced one or

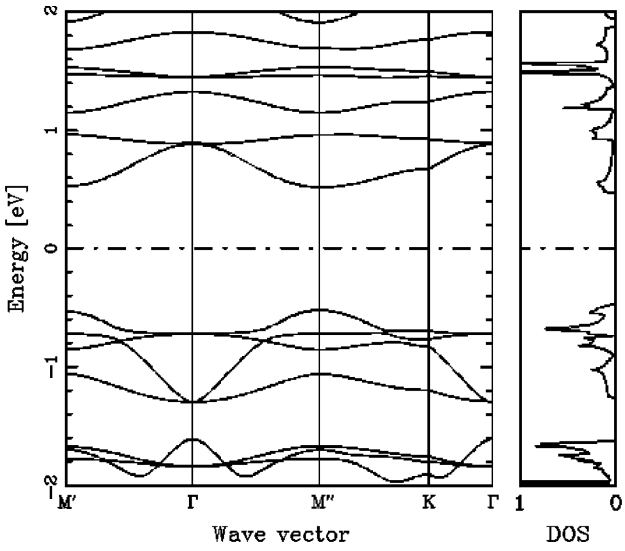

Fig. 21.2 Band structure (left) and electron DOS (right) for the defect-free Rh-C_{60}. The Fermi energy is set to zero.

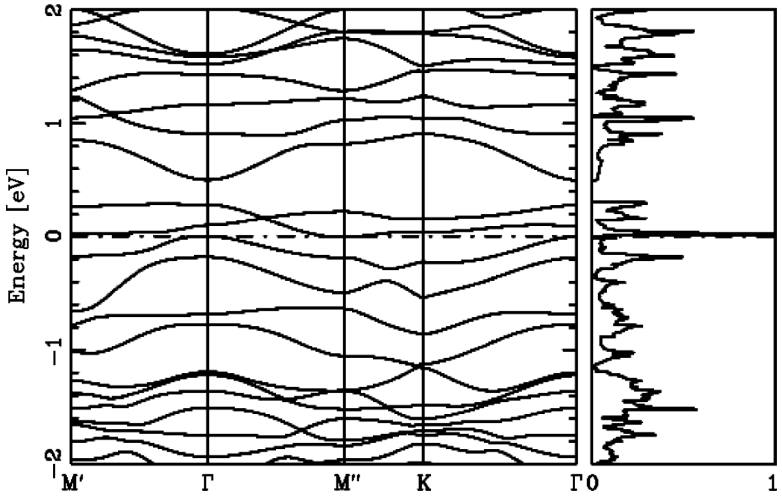

Fig. 21.3 Band structure and electron DOS for the defected Rh-C_{60} with one C_v per C_{60} molecule. The Fermi energy is set to zero.

both C_vs with one or two substitutional impurity atoms (IAs), respectively. We used non-magnetic IAs, namely N, B, P, O, S and repeated the same calculation using a capped SWCN consisting of 120 atoms instead of the C_{60} dimer (Andriotis *et al*. 2006b). Our results indicated that the impurity atoms do induce charge transfers, the direction of which depends on the relative electronegativity of the IA with respect to that of carbon. However, for every impurity investigated, it has been found that there is no induced spin localization associated with the IA. The spin density appears to be completely delocalized mainly over the carbon atoms of the C_{60} molecule, which includes the IA. If only one of the two C_vs of the C_{60} dimer is healed by an IA, the spin-density localization is restricted in the neighborhood of the remaining C_v. This leads us to conclude that none of the impurity atoms

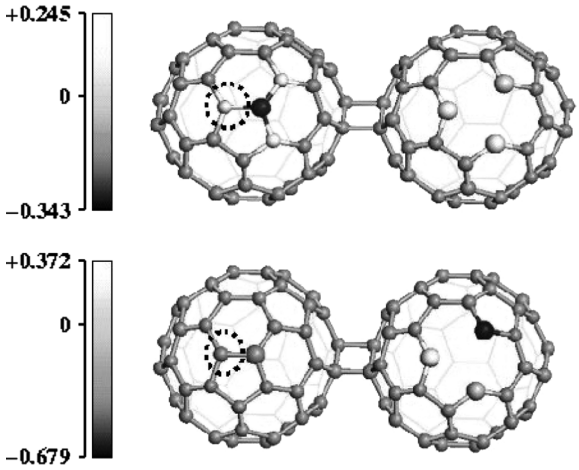

Fig. 21.4 Electron charge (top panel) and spin density (bottom panel) in a C_{60} dimer; One of the C_{60} molecules exhibits one C_v, while the other exhibits one substitutional N impurity. The positions of the impurity sites are within the indicated dotted circles.

studied can simulate the *charismatic* property of the C_v to promote spin localization in C-based materials. The latter is demonstrated in Fig. 21.4 that shows the electron charge (top panel) and spin (bottom panel) density for C_{60} dimer having one C_v (right molecule of Fig. 21.4) and one N impurity replacing the C_v in the other C_{60} molecule (left one in Fig. 21.4). Furthermore, it was also found that this property of the C_v is not affected in the presence of nearby carbon ad-atoms or distant substitutional impurity atoms.

21.3.3 Codoping

It is worth noting that the magnetism of the C_{60}-based polymers is associated with the presence of two kinds of defects, namely the C_vs and the $2+2$-cycloaddition bonds. According to the model proposed by Andriotis and collaborators, the development of sufficient interactions among the induced lone spins (or the embedded magnetic moments in the case of doping with TM atoms) is significantly facilitated (if this is not a requirement) if the system possesses two kinds of defects (of structural/topological or of substitutional impurity type) with one acting as a *donor* (D) and the other as an *acceptor* (A) crystal site. This seems to be a pre-requisite for the development and the stability of the defect-induced magnetism as was demonstrated in the case of carbon-based materials and the codoped Zn(Co,Cu)O (i.e. the ZnO system doped simultaneously with Co and Cu ions) (Andriotis *et al*. 2007, Janisch *et al*. 2005). More precicesly, the magnetic coupling in these materials was attributed to the *simultaneous presence* and the mediating character of the D- and the A-sites. Curiously, this is reminiscent, on the one hand, of Mc-Connell's theory of magnetism of charge-transfer magnetic salts (McConnell and Welch 1967) and, on the other hand, of the characteristics of the layered magnetic materials (Baibich *et al*. 1988, Samant *et al*. 1994).

The *simultaneous presence* of the two kinds of defects is nowadays referred to as a *codoped* state and the *codoping* was proposed as an alternative approach

to the induced magnetism in diluted magnetic semiconductors (DMSs) like the ZnO (Kuroda *et al*. 2007, Reed *et al*. 2005, Kittilstved *et al*. 2005, Ozaki *et al*. 2005, Kane *et al*. 2006, Ozaki *et al*. 2006, Dietl *et al*. 2000). Codoping has attracted attention from both experimental and theoretical researchers, primarily because of the possibility of using it to tailor the position and occupancy of the Fermi energy (E_F) of the doped DMSs and, thereby, to specify the occupancy of the density of states around E_F. Thus, codoping with shallow acceptors and donors was viewed as a potential means to specify the availability of carriers to mediate ferromagnetism (Kuroda *et al*. 2007, Reed *et al*. 2005, Kittilstved *et al*. 2005, Ozaki *et al*. 2005, Kane *et al*. 2006, Ozaki *et al*. 2006). A claim has also been made that the change of the charge state of the magnetic ions via codoping by shallow impurities may lead to the aggregation of the magnetic constituents (spinodal decomposition) rather than affecting the spin–spin interaction (Kuroda *et al*. 2007, Dietl *et al*. 2000).

21.4 Electronic, magnetic and transport properties

21.4.1 Defect-induced charge and spin transfer

In order to get a better understanding of the electronic and magnetic properties of the Rh-C_{60} polymer, we performed a series of *ab-initio* calculations using the GAUSSIAN-03 computer code (Gaussian 2003). We restricted these calculations to a C_{60} dimer in which the two C_{60} molecules are bonded by a $2 + 2$ cycloaddition bond. Detailed analysis of our results provided information about the charge and spin-density distribution in this system; they are presented in Figs. 21.5 and 21.6, respectively. Bonding and charge distribution on the bridge carbons and around the sites of the C_vs are shown in Fig. 21.5 along with the banana bonds (broken lines) that develop between two pairs of

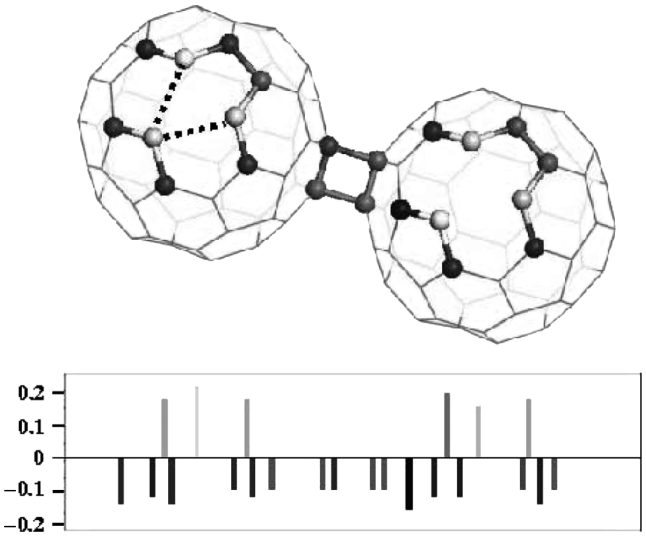

Fig. 21.5 Bonding and charge distribution on the bridge carbons and around the sites of the C_vs. The broken lines in this figure correspond to banana bonds that develop between two pairs of carbons atoms in one of the C_{60} monomers.

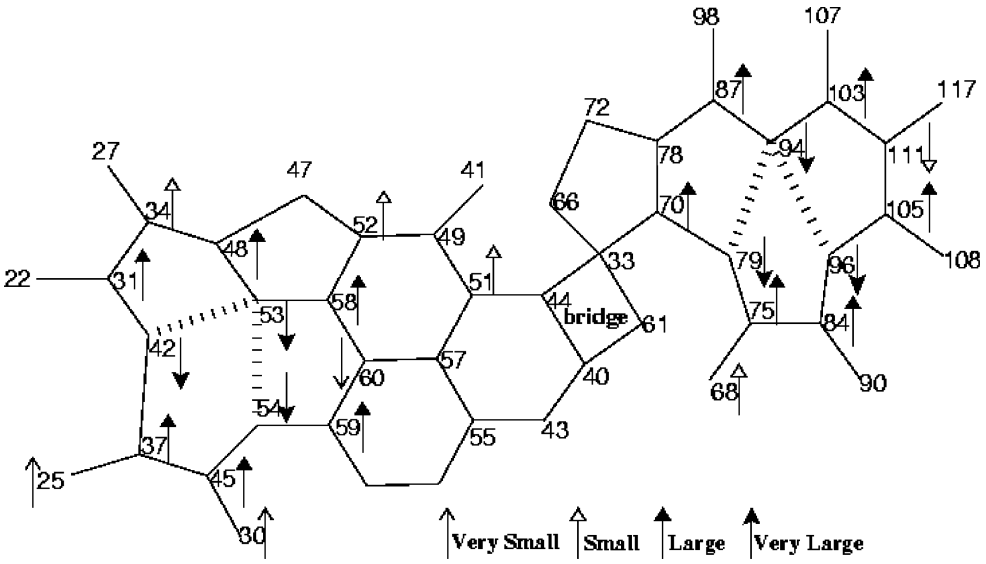

Fig. 21.6 Projected profile of the C_{60} dimer showing the spin-density distribution and the formulation of the SDW-like disturbance.

carbon atoms in one of the C_{60} monomers (see below). Figure 21.6 shows the projected profile of the C_{60} dimer showing the regions around the C_vs and the $2 + 2$ cycloaddition bond.

Two main characteristics of Fig. 21.5 are worth noting. The first is the structure around the C_v. This is not the same in the two defects (one surrounded by the C atoms 79, 94 and 96 and the other by the C atoms 42, 53 and 54 in Fig. 21.6) due to their inequivalent topology; they are located at different positions with respect to the $2 + 2$ cycloaddition bond. In the left vacancy site we observe the formation of pentagons and the development of *banana bonds*, similar to those formed in the C−C bonding in cyclopropane (Hamilton and Palke 1993). That is, upon the creation of a single vacancy by the removal of a carbon atom, the dangling bond that is generated on one of the carbon atoms adjacent to the vacancy site can subsequently form a bond with one of the other carbon atoms that was originally bonded to the vacant carbon atom. This decreases the distance between the two bonded carbon atoms, causing deformation of the ring structure and an increase in ring strain. Although the two carbon atoms are bonded, the ring deformation modifies the orbital overlap in such a way that it is intermediate between sigma-bonding and π-bonding. In cyclopropane, the bonding of three carbon atoms generates an equilateral triangular structure whose C−C−C bond angles are 60°. This is approximately 50° less than the optimal interorbital angle of 109.5° for sp^3 carbon. Consequently, the C−C bonding in cyclopropane is not truly sigma bonding in which the orbital overlap is end-on, nor is it truly π-bonding in which the orbital overlap is lateral, but is instead a bond arising from a type of bent overlap intermediate between σ and π bonding. This type of C−C bond formation is found also in the region around the C_vs of the C_{60} dimer. The second characteristic is the distribution of the electron density, which exhibits

a perturbation in the form of a CDW-like modulation. This is the result of defect-induced charge transfers leading to the development of large EDMs. Assigning the ferromagnetic coupling among the induced magnetic moments to the strong electric fields developed by the induced EDMs, this picture makes it apparent why the presence of two kinds of defects that can act as donors and acceptors, respectively, can facilitate the magnetic coupling.

A corresponding modulation in a SDW-like form was also found in the electron spin density as shown in Fig. 21.6. It is worth emphasizing that there is a high degree of localization of the spin density (indicated by the large spin-vectors) around the carbon vacancies that decays quickly in the form of Friedel oscillations.

21.4.2 Remote selective delocalization

In order to examine in more detail the defect-induced electron charge and spin transfers, we checked the contribution of the atomic orbitals (AOs) to the molecular orbitals (MOs) of the C_{60} dimer in three cases: (i) the singlet state of the defect-free case, (ii) singlet state and (iii) the triplet state, the latter two for the defected configuration, i.e. the state in which there is one C_v in each C_{60} molecule. Representative results from these calculations are included in Figs. 21.7 and 21.8. In these, the x-axis indicates the numbering of the 120 atoms of the C_{60} dimer. The y-axis indicates the contributions to the highest-occupied MOs (HOMOs), namely the HOMO$-k$; $k = 0, 1, 2, 3, 4, 5$, and the lowest-unoccupied MOs (LUMOs), namely the LUMO $+ k$; $k = 0, 1, 2, 3, 4, 5$; (the $k = 0$ cases refer to HOMO and LUMO levels, respectively). For example, if a contribution is found of the mth-AO (m2[1,120]) to the HOMO-l MO, this is shown in the figure by a symbol at the point (m, HOMO-l). For presentation purposes, the results have been shifted higher or lower from the $y = k$ lines. As can be observed from these figures, the singlet states are characterized by an extended delocalization. Each of the shown HOMO$-k$ and the LUMO $+ k$ are built by contributions from almost all the AOs. In contrast

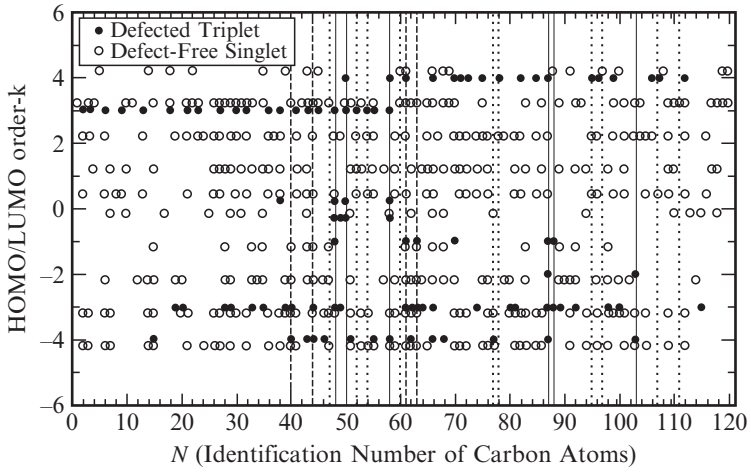

Fig. 21.7 Site occupation of the LUMO $+ k$ and HOMO$-k$, $k = -4, -3, -2, -1, 0, 1, 2, 3, 4$, of spin-up electrons in the defect-free singlet (open circles shifted slightly relative to the $k = -4, -3, -2, -1, 1, 2, 3, 4$ lines for clarity of presentation) and defected triplet (solid circles) state for the C_{60} dimer with one C_v per C_{60} molecule. The $k = 0$ MOs are also shifted relative to the $k = 0$ line. Carbon atoms surrounding the vacant sites ($N = 48$, 50, 58, 87, 88, 103) are indicated by the perpendicular solid lines, while sites that are second nearest neighbors to the vacant sites are indicated by the dotted perpendicular lines. Dashed lines indicate C atoms participating in the $2 + 2$ cycloaddition bond.

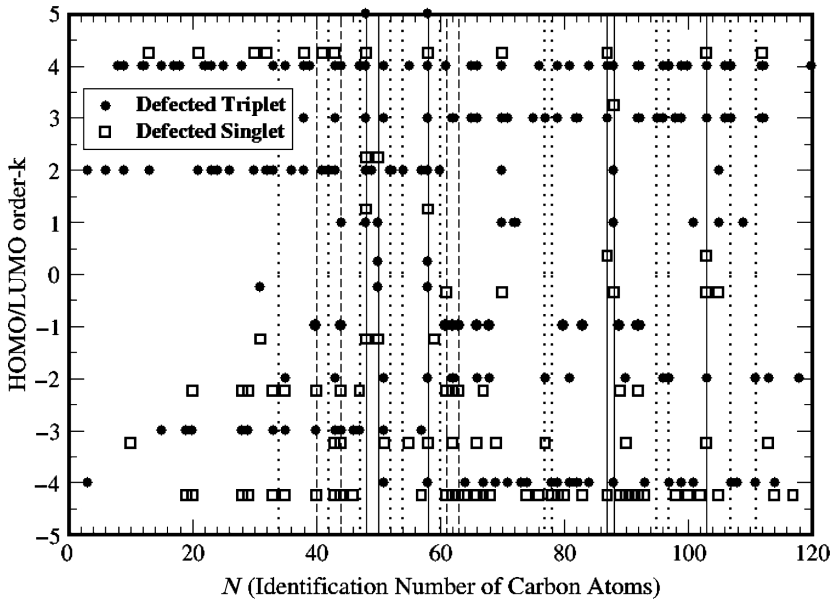

Fig. 21.8 The same as in Fig. 21.7 but for for spin-down electrons and for the defected singlet (open squares) and defected triplet states of the C_{60} dimer with one C_v per C_{60} molecule.

with this picture, the MOs of the defected C_{60} dimer are usually formed from pronounced contributions from certain AOs and, preferably, from those around the defect sites indicated by the perpendicular lines. These results make it clear that C_vs act as sites that are provided for the development of a *selective and remote delocalization* of the electron and spin density. As was shown in Section 21.3.2, the substitutional impurities do not share both of these features; while they induce charge localization, they induce a delocalization of the spin density.

21.4.3 Anisotropy and distance dependence of exchange coupling

A measure of the exchange coupling between the magnetic moments can be obtained by calculating the energy difference between the triplet and singlet states. In Table 21.1, results are presented for the C_{60} dimer (with one C_v per C_{60} molecule) at various symmetry configurations and the linear C_{60} trimer, the latter containing two C_vs, one each on its end C_{60} molecules (see Fig. 21.9).

In the case of the C_{60} dimer, the C_vs are put at sites of *cis* and *trans* configurations (see Fig. 21.9) as well as in one at right angles to each other (i.e. on lines perpendicular to each other and to the line passing through the centers of the C_{60} molecules). Our results, shown in Table 21.1, indicate moderate anisotropy in the exchange interaction. The trends found in our detailed investigation in the above-described C_{60} dimer were reconfirmed in the case of the linear C_{60} trimer in which the two end C_{60} molecules contain one C_v (Fig. 21.9). For this system, the ground state appears to be also the triplet state. From these calculations we get the information for the dependence of the exchange coupling on the distance between the magnetic moments.

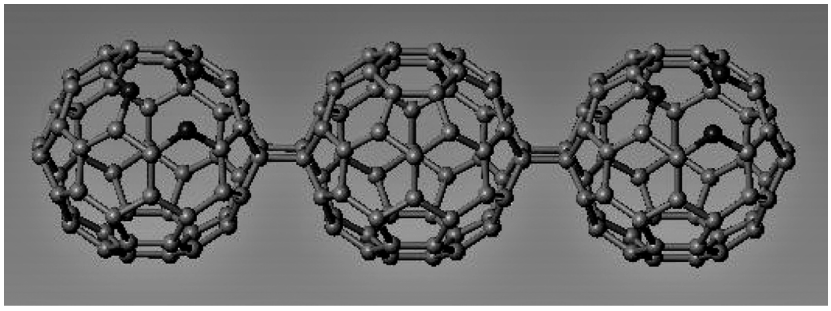

Fig. 21.9 A C_{60} trimer; each of the outer C_{60} molecules (left and right) exhibit one C_v (located among the dark-colored atoms).

Finally, comparing the results of the C_{60} trimer to that of the C_{60} dimer, it is observed that the exchange coupling between the lone spins (localized at the vacancy sites in both systems), although weaker in the trimer case, is still strong enough to support our proposed explanation that the ferromagnetic coupling is the result of the remote delocalization and the associated remote overlaps among the MOs.

21.4.4 Transport properties

We have also examined the transport properties of the two-dimensional Rh-C_{60} polymer by calculating the current–voltage (I–V) characteristic curves of a finite part of this polymer (see Fig. 21.11). Our calculation is based on the surface Green's function matching method (SGFMM) (Andriotis and

Table 21.1 The energy difference between triplet and singlet state of the C_{60} dimer and C_{60} trimer at various symmetry configurations (see Fig. 21.10 for clarifying *cis* and *trans* symmetries).

Structure	Symmetry	E(triplet)-E(singlet) (meV)
$[C_{60}]_2$	*cis*	−790
$[C_{60}]_2$	*trans*	−790
$[C_{60}]_2$	at right angle	−620
$[C_{60}]_3$	*cis*	−470

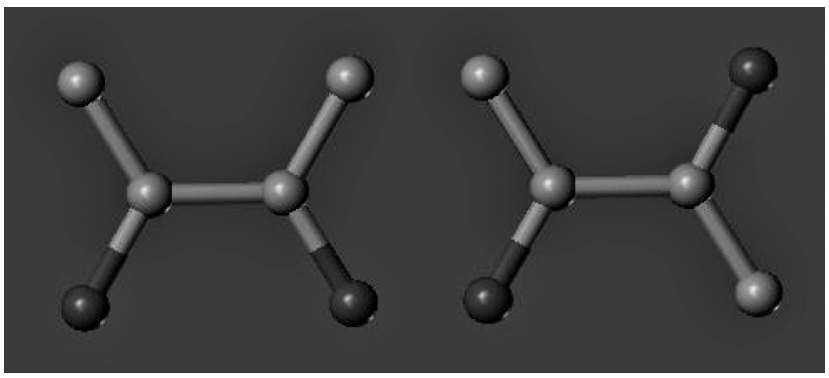

Fig. 21.10 Schematic presentation of *cis* (left) and *trans* (right) symmetry configurations. The carbon atoms are shown in light, while the impurity atoms are shown in dark.

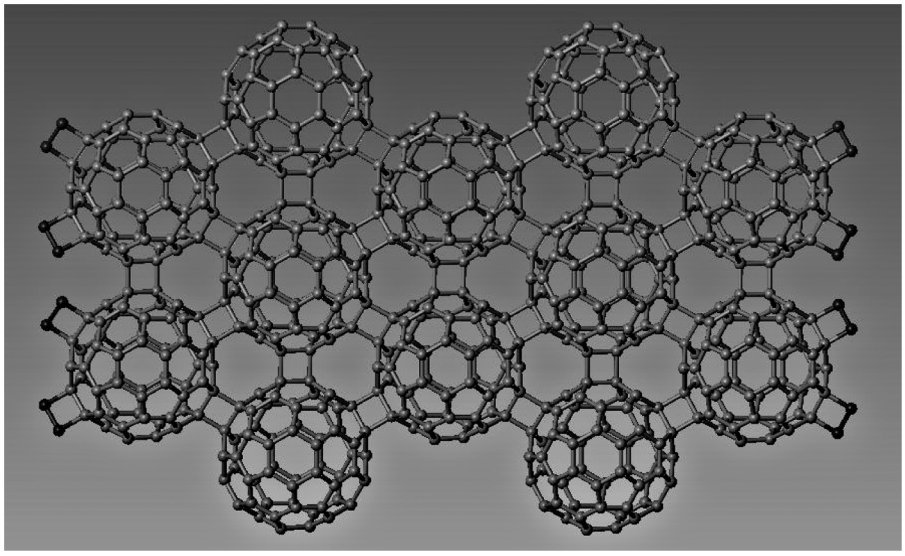

Fig. 21.11 A finite part of the two-dimensional Rh-C_{60} polymer used in the transport calculation. Atoms highlighted in dark indicate the atoms in contact with the metal leads.

Menon 2001). In this approach we follow Datta's formalism (Datta 1995) suitably modified by implementing it in the embedding approach of Inglesfield and Fisher (Andriotis 1992, 1990). In particular, the transmission function $T(E, V_\mathrm{b})$ at the applied voltage V_b is calculated firstly according to the expression:

$$T(E, V_\mathrm{b}) = \mathrm{tr}\left[\Gamma_\mathrm{L} G_\mathrm{C} \Gamma_\mathrm{R} G_\mathrm{C}^\dagger\right], \tag{21.1}$$

where

$$\Gamma_j(E; V_\mathrm{b} = i\left(\sum\nolimits_j - \sum\nolimits_j^\dagger\right), \quad j = \mathrm{L}, \mathrm{R}, \tag{21.2}$$

and G_C is the Green's function of the conducting tube obtained as follows (Datta 1995):

$$G_\mathrm{C} = \left(\mathrm{E} - H_\mathrm{C} - \sum\nolimits_\mathrm{L} - \sum\nolimits_\mathrm{R}\right)^{-1}, \tag{21.3}$$

where H_C is the Hamiltonian of the isolated tube and $\sum_\mathrm{L}$, $\sum_\mathrm{R}$ the left (L) and right (R) self-energies that incorporate the effect of the tube contacts with the metallic leads. With the symbol $T(E)$ we will denote the transmission function at zero bias, i.e. $T(E) = T(E,\ V_\mathrm{b} = 0)$.

In the tight-binding formulation used in the present work both the Hamiltonians and the Green's functions are each taken to be $N_\mathrm{at}N_\mathrm{orb} \times N_\mathrm{a}tN_\mathrm{orb}$ matrices, where N_at is the number of atoms in the embedding subspace and N_orb is the number of orbitals on each atom. We use $N_\mathrm{orb} = 9$ that includes 1-s, 3-p and 5-d orbitals for C and the metal-lead (the latter taken to be a 3-d transition metal).

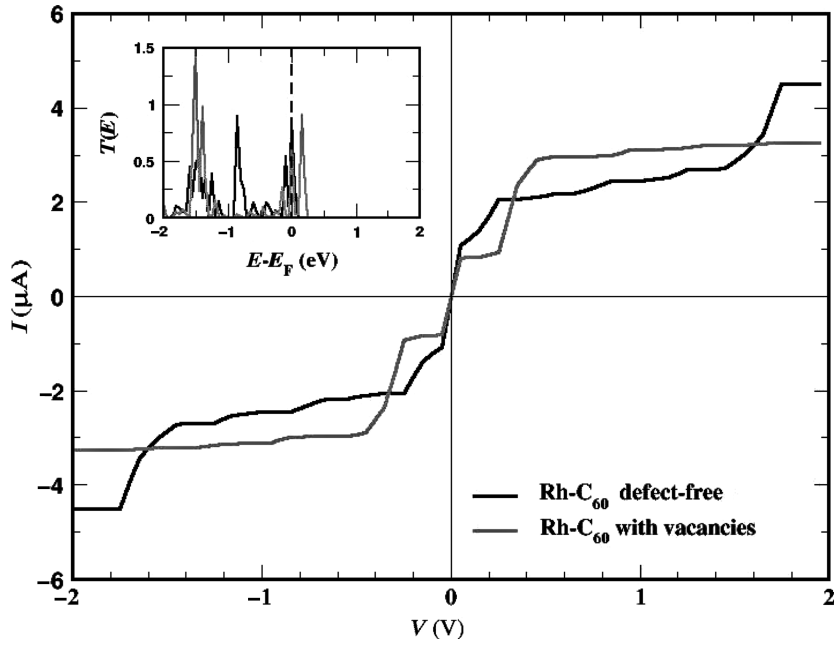

Fig. 21.12 The *I–V* characteristic of the structure shown in Fig. 21.11; the dark curve corresponds to a defect-free structure; the dashed or dotted curve to a defected structure in which each C_{60} molecule contains one C_v. In the inset, the corresponding transmission functions are shown in units of $(\frac{2s^2}{k})$. The Fermi energy is set to zero.

Finally, the evaluation of the current–voltage, *I–V*, characteristic of the tube is performed by utilizing the following formula: (Datta 1995)

$$I(V_b) = \tfrac{2e}{h} \int_{-\infty}^{+\infty} T(E, V_b)[f_E(\mu_L) - f_E(\rho_E)]\, dE, \qquad (21.4)$$

where $\mu_i = E_F - eV_i$; $i = L, R$, V_L and V_R are the applied voltages on the left and the right metal leads, respectively, $e > 0$ is the electron charge, E_F the Fermi energy of the free tube and $f_E(\mu)$ the Fermi distribution. We define $V_b = V_L - V_R$ to be the bias voltage.

The same tight-binding Hamiltonian is used both in the conductivity calculation as well as for performing molecular-dynamics simulations for structural relaxation ensuring consistency in the calculations. We consider both the defect-free Rh-C_{60} as well as the defected one containing one C_v per C_{60} molecule.

In the inset of Fig. 21.12 we show the calculated transmission function $T(E)$ for the two cases. As can be observed, there are no conduction channels above the Fermi energy (set to zero) in the defect-free system. The presence of C_vs introduces more transport channels, some of which extend above the Fermi energy. The main part of Fig. 21.12 shows the corresponding *I–V* curves for the two cases. As is apparent from this figure, the defects (C_vs) lead to an increase in the current due mainly to the creation of new conduction channels below and above the Fermi energy as well as to the narrowing of the electron gap.

21.5 Magnetic coupling among magnetic moments

As stated above, it appears that a consensus has been reached regarding the origin of the magnetic moments in C-based materials; that this is induced by structural, topological and impurity defects. The unresolved issue, however, pertains to how these magnetic moments are coupled ferromagnetically. The ferromagnetic coupling among the defect-induced magnetic moments is not only a local effect due to the point-group symmetry of the defect site, the band splitting, and the band-filling factors of the atomic orbitals of the surrounding defect (and/or the impurity) atoms (and/or ligands) (Mpourmpakis *et al*. 2003, 2005). These features, while playing a primary role in the formation of the magnetic moments, also contribute to the development of the magnetic coupling either in a direct or indirect way. However, the ferromagnetic coupling among neighboring magnetic moments depends crucially on their mutual interaction that, in turn, is established by the induced charge transfers. That is, it depends strongly on the electron–electron (*e*-*e*) correlations and as previously discussed (see details in Sections 21.2 and 21.3), the way *e*-*e* correlations promote the magnetic coupling can be viewed from different angles.

Q5 McConnell (1967) attributed the ferromagnetic coupling to the kinetic exchange, i.e. a contribution to CI (see Section 21.5.1). Similarly, other researchers rely on the CI approach in order to explain it. On the other hand, most of the efforts concerning this investigation are based on SRMs because (as we have already discussed) of their simpler and computationally tractable formalism.

In the following, we make a more detailed reference to the proposed CIMs and discuss the way we mapped our SRM results onto a generalization of the McConnell model. As will be shown, this generalization is not only applicable to the C-based materials but also to the doped NTIMs as well.

21.5.1 Kinetic exchange

Strictly speaking, the kinetic exchange interaction is a configuration interaction (CI) term that plays an important role in chemical bonding. In a simplistic scenario it can be viewed as the outcome of quantum interference effects among the basic set functions (for example, atomic orbitals (AOs)) which are used to describe the molecular orbitals (MOs) (for a recent discussion see, for example, (Yamaguchi *et al*. 2006) and references therein). This is played out in Anderson's Hamiltonian, namely in the description of a magnetic (impurity) atom embedded into a non-magnetic metallic host (Anderson 1961) in which a single electron state is described in terms of Bloch functions of the host lattice and *d*-type AOs of the magnetic impurity. This model formed the basis for the study of the diluted magnetic semiconductors (DMSs).

Q6 As shown by Schrieffer and Wolff (1966), Anderson's Hamiltonian (Anderson 1961) can be transformed into the form of an $s-d$ exchange model in which two fundamental interaction mechanisms (between a valence electron and the magnetic impurity) prevail (Larson *et al*. 1988, Blinowski

and Kacman 1992). One of them is an energy-dependent exchange interaction, $J_{kk'}$, of negative sign (i.e. of antiferromagnetic (AF) order). The other is a spin-independent direct $s-d$ exchange interaction (Scgrieffer and Wolff 1966). The former is known as the *kinetic exchange* interaction and within the k-space perturbation theory it can be viewed as originating from the virtual transitions of a conduction electron between the conduction *sp*-bands and the d or f bands of the magnetic impurity. Later considerations have shown that depending on the band filling of the d-band and the spin multiplicity of the ground state of the magnetic ion, the kinetic exchange can be of AF or FM Kondo-like or exhibiting a more complicated form (Blinowski *et al*. 1996).

In the presence of more than one magnetic ions embedded in a non-magnetic host the kinetic exchange interaction is expected to play a key role in their mutual interaction. That is, a significant part of the polarization experienced by the conduction electron in the neighborhood of the magnetic ion is attributed to the kinetic exchange that, in turn, affects the indirect interaction between the magnetic ions. In view of this picture the kinetic exchange interaction is expected to play a crucial role in the description of mediated exchange interactions as, for example, the superexchange and the double-exchange interactions.

It is apparent that the perturbative computation of the kinetic exchange requires a knowledge of the whole spectrum (and the corresponding wavefunctions) of the Hamiltonian of concern. The knowledge of the excited states is a pre-requisite for the calculation of the kinetic exchange; it is a consequence of the single-configuration approximation (and the single-electron approximation) of the solution that is looked upon. It may be possible, however, to avoid the single-electron perturbative approach to the kinetic exchange and limit the number of the excited single-electron states needed for its calculation. This may be achieved by attempting a multiconfigurational description of the electronic states of the DMSs, while keeping only a few Slater determinants (configurations), namely those that can guarantee the capture of the major part of the correlation effects. In such a procedure, the kinetic exchange will be the result of interference terms among the various molecular configurations used in the construction of the many-electron wavefunctions and is inherently incorporated within the calculated total energy. As characteristic examples of multiconfigurational approaches we point out the following:

- The organic charge-transfer salts consisting of alternating donor (D) and acceptor (A) sites viewed as alternating D–A chains extending all over the material. In these, it may be possible for the triplet state of a neutral D–A dimer (D^0A^0, participating in a D–A chain) to induce a triplet state of their charge-transfer configuration (D^+A^-) through a CI, with the latter facilitated by the electric fields developed by the charge-transfer processes. This triplet state is then propagated along the D–A chain as suggested by McConnell (McConnell and Welch 1967). Therefore, in such an approach two multielectron configurations, namely D^0A^0 and D^+A^-, are involved in the CI formulation of the problem (see Fig. 21.13) and associated with them the kinetic exchange results from their interference.

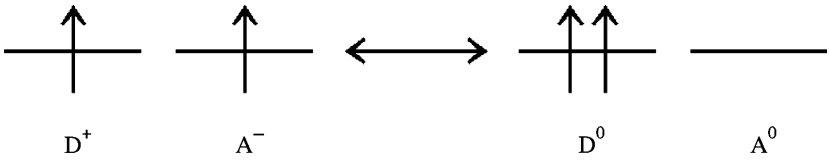

Fig. 21.13 Schematic representation of McConnell's CI approach (McConnell and Welch 1967).

- The superexchange model of Kramers and Anderson for antiferromagnetism as applied to MnO (Kramers 1934, Anderson 1950). In this, the wavefunction of the system is written in terms of two MOs, namely the ground-state MO and an excited MO. In the former, the O atom mediating the interaction of two Mn atoms that are its first nearest neighbors has two antiparallel electrons. The latter is a *charge-transfer state* in which one electron from the oxygen atom moves onto one of the Mn atoms.
- The double-exchange model of Anderson–Hasegawa (1955) proposed for explaining the origin of ferromagnetism in the mixed-valence manganites of perovskite structure (Anderson and Hasegawa 1955). In this, three MO configurations are constructed by combining the most probable atomic (electronic) configurations of one oxygen atom and its two neighboring Mn ions by taking into account the spin multiplicity of each constructed MO. Here, once again, the charge-transfer states are essential and are included in the CI approach.
- The consideration of van Vleck of Ni ferromagnetism (van Vleck 1953).

Q7

21.5.2 Generalized McConnell model

In Section 21.1, it was pointed out that features similar to those found in the magnetic C_{60}-based polymers were also identified in some of the magnetic doped-NTIMs. These observations led us to propose that these two different classes of materials belong to the same class of magnetic materials whose magnetism is due to defects (Andriotis and Menon 2005, Andriotis *et al*. 2003, 2005a, 2005b, 2007, 2006a). The similarities between these two classes of materials pertain mainly to the development of the ferromagnetic coupling among the magnetic moments that in the C-based materials are induced by the defects, while in the class of the doped-NTIMs are provided by the impurity atoms (either magnetic or non-magnetic). In both classes, however, the magnetic moments are induced by the defects (either of intrinsic or extrinsic type). The model we proposed in order to explain the origin of this defect-induced magnetism is a generalization of McConnell's theory (McConnell and Welch 1967). According to our proposal, the presence of two kinds of defects (of donor and acceptor type, respectively) is necessary in order to promote positive- and negative-charge and spin-density localizations, self-sustained by the development of strong electric fields. A schematic view of our proposal is shown in Fig. 21.14. According to this, the defects provide locations for localizing separately the induced positive and negative charge transfers shown as light and dark shaded neighborhoods in the system. In any or both of these localization regions, electron spin density is also localized, forming the

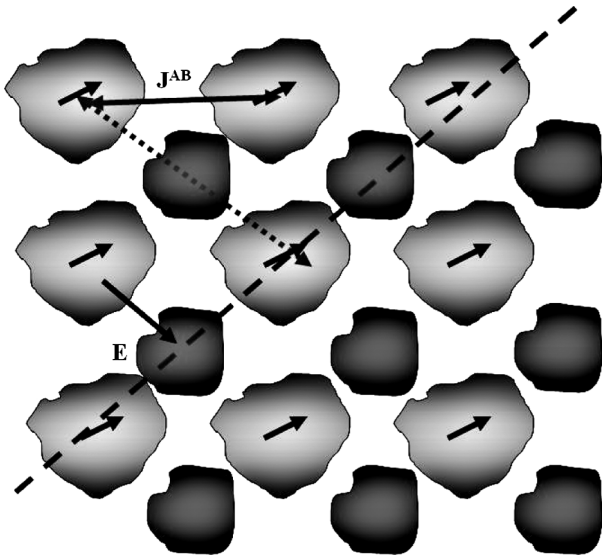

Fig. 21.14 Pictorial view of a magnetic system described in terms of electron charge transfers leading to locally positive and negative regions (as shown by light- and dark-shaded regions, respectively) as well as spin-density transfers leading to the formation of magnetic moments (indicated by arrows). The charge localizations are organized in periodic arrays of donor (D) and acceptor (A) regions.

magnetic moments (shown with the short arrows). This settlement (which is not necessary to be periodic as in Fig. 21.14), leads to the development of the electric fields (shown by E in the figure) which, in turn, establish the ferromagnetic coupling (shown as J^{AB}) among the magnetic moments.

It is understood that the details for the formation of the magnetic moments is mostly *system specific*, depending on the defect types, the point group symmetry of their location in the crystal, the band splitting and fillings of the AOs associated with the atoms in the neighborhood of the defects, etc. However, it is strongly affected by the electronic structure of the (host) material (bandgap, spin polarization and position of spin states relative to the gap, impurity levels, etc.).

The exchange coupling among the magnetic moments appears to be associated with the remote delocalization and overlap of the MOs both of which are induced by the C_vs as this was sufficiently discussed in Section 21.4.2. In this, it was shown that the delocalization is remote and selective, establishing, thus, remote overlap among the MOs. It is this remote overlap that contributes to the exchange coupling among the magnetic moments. A characteristic example appears to be the case of the C_{60} trimer (shown in Fig. 21.9). In this view, and at least on the nanoscale, doping concentrations smaller than the percolation threshold can lead to ferromagnetism. Therefore, metallicity seems not to be a pre-requisite for the establishment of magnetism. Nevertheless, as we have seen, defects eliminate the electron energy gap of the two-dimensional Rh-C_{60} polymer as demonstrated in Fig. 21.3.

21.5.3 Similarities with magnetic non-traditional inorganic materials

The similarities that we identified between the magnetic features of the C_{60}-based polymers and those of the NTIMs made us check our model proposal in

the case of the ZnO codoped with two kinds of substitutional impurities that can act as donor and acceptor sites. In particular, we studied the ZnO codoped with Co^{2+} and Cu^{+} ions (to be denoted as Zn(Co,Cu)O). Our preliminary results have indicated that, in agreement with Fig. 21.14, one of the defects (Co) provides mainly the magnetic moments, while the other acts as a ferromagnetic coupling mediator even at distances as long as 3rd nearest neighbors in the Zn sublattice. Interestingly, it was found that a ferromagnetic coupling between the Co ions is established if the Cu atom intervening between is spin polarized, a picture reminiscent the RKKY interaction (Ruderman and Kittel 1954, Kasuya 1956, Yosida 1957) between magnetic ions embedded in a metal (Lathiotakis *et al*. 2008).

21.6 Conclusion

The defect-induced ferromagnetism in C-based materials is an exciting and challenging phenomenon. It has attracted intense efforts in recent years and many models have been proposed soon after its observation. From the results of the present work and other reported ones, it has become clear that two interrelated but, in many aspects, mutually independent processes are responsible for its development. One of these processes has mainly local character. It is associated with the development of the magnetic moments. It depends on the type of the defect, its point-group symmetry, its ligand fields and the type and band filling of the ligand AOs. These factors specify the electron charge and spin transfers towards or away from the defect region; they are affected by the electronic structure of the host material. The second process establishes the ferromagnetic coupling among the induced magnetic moments. This is mainly based on the strength of the electrostatic fields that are developed by the charge transfers. As our calculations have shown, in the C_{60}-based polymers, the C_vs and the $2+2$ cycloaddition bonds are indeed responsible for the development of large electrostatic dipole moments. These are responsible for large electric fields that, in turn, enable the defect sites to retain the charge and spin localization in their region. This picture is reminiscent of McConnell's model for ferromagnetism in the magnetic organic salts and allows us to propose a generalization of it as a possible mechanism for the defect-induced carbon ferromagnetism. Our generalization considers the presence of two kinds of defects, which can act as donor and acceptor sites, respectively, as a necessary pre-requisite for the occurrence of magnetism. This defect combination ensures the presence of charge neutrality and can lead to the necessary development of the electric fields that will promote the charge localization. The proposed generalization is not limited solely to the role of the kinetic exchange interaction. All CI contributions have their share in this phenomenon. We have arrived at this conclusion based on our numerical results that revealed large defect-induced charge transfers and, associated with them, large electric fields, both of which were found to promote the triplet state configuration as the energetically most favorable one for the ground state. Finally, it is worth noting that further investigations led us to the observation that the proposed explanation of the carbon magnetism is equally well applicable in the case

of doped-NTIMs that, as demonstrated, do indeed exhibit those characteristic features that underline the magnetism of the C-based materials.

Acknowledgements

The present work is supported through grants by DOE (DE-FG02-00ER45817 and DE-FG02-07ER46375) and US-ARO (W911NF-05-1-0372).

References

Anderson, P.W. *Phys. Rev*. **79** 350 (1950). **Q8**

Anderson, P.W. *Phys. Rev*. **124** 41 (1961).

Anderson, P.W. and Hasegawa, H. *Phys. Rev*. **100** 675 (1955).

Andriotis, A.N. *J. Phys. Condens. Matter* **2** 6079 (1990).

Andriotis, A.N. *Europhys. Lett*. **17** 349 (1992).

Andriotis, A.N., Fthenakis, Z.G. and Menon, M. *Europhys. Letters* **76** 1088 (2006a).

Andriotis, A.N. and Menon, M. *Phys. Rev. B* **57** 10069 (1998).

Andriotis, A.N. and Menon, M. *J. Chem. Phys*. **115** 2737 (2001).

Andriotis, A.N. and Menon, M. *Phys. Rev. Lett*. **93** 026402 (2004).

Andriotis, A.N. and Menon, M. Clusters and Nano-assemblies: Physical and Biological Systems, (ed. Jena, P., Khanna, S.N. and Rao, B.K.) (World Scientific, Singapore, 2005)

Andriotis, A.N., Menon, M. and Froudakis, G.E., *Phys. Rev. B* **62** 9867 (2000).

Andriotis, A.N., Menon, M., Froudakis, G.E., Fthenakis, Z. and Lowther, J.E. *Chem. Phys. Lett*. **292** 487 (1998).

Andriotis, A.N., Menon, M., Froudakis, G.E. and Fthenakis, Z. *Chem. Phys. Lett*. **301** 503 (1999).

Andriotis, A.N., Menon, M., Sheetz, R.M. and Chernozatonskii, L. *Phys. Rev. Lett*. **90** 026801 (2003).

Andriotis, A.N., Menon, M., Sheetz, R.M. and Richter, E. Carbon based magnetism, (ed. Makarova, T.L. and Palacio, F.), (Elsevier 2006a) p.483.

Andriotis, A.N. and Srivastava, D. *J. Chem. Phys*. **117** 2836 (2002).

Andriotis, A.N., Sheetz, R.M., Lathiotakis, N.N. and Menon, M. *Int. J. Nanotechnol*. (to appear) (2007). **Q9**

Andriotis, A.N., Sheetz, R.M. and Menon, M. *J. Phys.: Condens. Matter* **17** L35 (2005a).

Andriotis, A.N., Sheetz, R.M. and Menon, M. *Phys. Rev. B* **74** 153403 (2006b).

Andriotis, A.N., Sheetz, R.M., Richter, E. and Menon, M. *Europhys. Lett*. **72** 658 (2005b).

Baibich, M.N., Broto, J.M., Fert, A., Nguyen Van Dau, F., Petroff, F., Eitenne, P., Creuzet, G., Friederich, A. and Chazelas, J. *Phys. Rev. Lett*. **61** 2472 (1988).

Blinowski, J. and Kacman, P. *Phys. Rev. B* **46** 12298 (1992).

Blinowski, J., Kacman, P. and Majewski, J. A. *Phys. Rev. B* **53** 9524 (1996).

Bouzerar, G. and Ziman, T. *Phys. Rev. Lett*. **96** 207602 (2006).

Chan, J.A., Montanari, B., Gale, J.D., Bennington, S.M., Taylor, J.W. and Harrison, N.M. *Phys. Rev. B* **70** 041403(R) (2004).

Datta, S. *Electronic transport in mesoscopic systems*, Cambridge University Press, Cambridge (1995).

Dietl, T. *Nature Mater*. **5** 673 (2006).

Dietl, T., Ohno, H., Matsukura, F., Cibert, J. and Ferrand, D. *Science* **287** 1019 (2000).

El-Barbary, A.A., Telling, R.H., Ewels, C.P., Heggie, M.I. and Briddon, P.R. *Phys. Rev. B* **68** 144107 (2003).

Fink, K. *Chem. Phys*. **326** 297 (2006).

Fthenakis, Z., Andriotis, A.N., and Menon, M. *J. Chem. Phys*. **119** 10911 (2003).

Gaussian 03, Revision A.1, Frisch, M.J. et al., Gaussian, Inc., Pittsburgh PA (2003).

Hamilton, J.G. and Palke, W.E. *J. Am. Chem. Soc*. **115** 4159 (1993).

Harigaya, K. *Chem. Phys. Lett*. **340** 123 (2001).

Harigaya, K. and Enoki, T. *Chem. Phys. Lett*. **351** 128 (2002).

Hjort, M. and Stafstrom, S. *Phys. Rev. B* **61** 14089 (2000).

Janisch, R., Gopal, P. and Spaldin, N.A. *J. Phys.: Condens. Matter* **17** R657 (2005).

Kane, M.H., Strassburg, M., Fenwick, W.E., Asghar, A., Payne, A.M., Gupta, S., Song, Q., Zhang, Z.J., Dietz, N., Summers, C.J and Ferguson, I.T. *J. Cryst. Growth* **287** 591 (2006).

Kasuya, T. *Prog. Theor. Phys*. (Kyoto) **16** 45 (1956).

Kim, Y.-H., Choi, J., Chang, K.J. and Tomanek, D. *Phys. Rev. B* **68** 125420 (2003).

Kittilstved, K.R., Norberg, N.S. and Gamelin, D.R. *Phys. Rev. Lett*. **94** 147209 (2005).

Kramers, H.A. *Physica* **1** 182 (1934).

Kuroda, S., Nishizawa, N., Takita, K., Mitime, M., Bando, Y., Osuch, K. and Dietl, T. *Nature Mater*. **6** 440 (2007).

Larson, B.E., Hass, K.C., Ehrenreich, H. and Carlsson, A.E. *Phys. Rev. B* **37** 4137 (1988).

Lathiotakis, N N., Andriotis, A.N. and Menon, M. (submitted for publication) (2008).

Lathiotakis, N N., Andriotis, A.N., Menon, M. and Connolly, J. *J. Chem. Phys*. **104** 992 (1996).

Lehtinen, P.O., Foster, A.S., Ayuela, A., Krasheninnikov, A., Nordlund, K. and Nieminen, R.M. *Phys. Rev. Lett*., **91** 017202 (2003).

Lehtinen, P.O., and Foster, A.S., Ma, Y., Krasheninnikov, A.V. and Nieminen, R.M. *Phys. Rev. Lett*. **93** 187202 (2004).

Makarova, T.L. Studies of High-Tc Superconductivity, (ed. Narlikar, A.) abstract cond-mat/0207368. Vol. **44–45**.

Makarova, T.L., Sundquist, B., Hohne, R., Esqulnazi, P., Kopelevich, Y., Scharff, P., Davidov, V.A., Kashevarova, L.S. and Rakhmanlna, A.V. *Nature* **413** 716 (2001).

Marques, L., Mezouar, M., Hodeau, J.-L. and Nunez-Regueiro, M. *Phys. Rev. B* **68** 193408 (2003).

Matsumoto, Y., Murakami, M., Shono, T., Hasegawa, T., Fukumura, T., Kawasaki, M., Ahmet, P., Chikyow, T., Koshihara, S. and Koinuma, H. *Science* **291** 854 (2001).

McConnell, H.M. and Welch, Proc. R.A. *Found. Chem. Res*. **11** 144 (1967).

Menon, M. *J. Phys.: Condens. Matter* **10** 10991 (1998).

Mpourmpakis, G., Froudakis, G.E., Andriotis, A.N. and Menon, M. *Phys. Rev. B* **68** 125407 (2003).

Mpourmpakis, G., Froudakis, G.E., Andriotis, A.N. and Menon, M. *Phys. Rev. B* **72** 104417 (2005).

Narymbetov, B., Omerzu, A., Kabanov, V.V., Tokumoto, M., Kobayashi, H. and Michailovic, D. *Nature* **407** 883 (2000).

Nicolaides, C.A., Zdetsis, A.D. and Andriotis, A.N. *Solid State Commun*. **50** 857 (1984).

Okotrub, A.V., Belavin, V.V., Bulusheva, L.G., Davydov, V.A., Makarova, T.L. and Tomanek, D. *J. Chem. Phys*. **115** 5637 (2001).

Onoe, J. and Takeuchi, K. *Phys. Rev. Lett*. **79** 2987 (1997).

Osorio-Guillen, J., Lany, S., Barabash, S.V. and Zunger, A. *Phys. Rev. Lett*. **96** 107203 (2006).

Ovchinnikov, A.A. *Theor. Chimica Acta* **47** 297 (1978).

Ovchinnikov, A.A., Shamovsky, I.L. *J. Mol. Structure* (Theochem) **251** 133 (1991).

Ozaki, N., Nishizawa, N., Marcet, S., Kuroda, S., Eryu, O. and Takita, K. *Phys. Rev. Lett*. **97** 037201 (2006).

Ozaki, N., Okabayashi, I., Kumekawa, T., Nishizawa, N., Marcet, S., Kuroda, S. and Takita, K. *Appl. Phys. Lett*. **87** 192116 (2005).

Park, C.H. and Chadi, D.J. *Phys. Rev. Lett*. **94** 127204 (2005).

Reed, M.J., Arkun, F.E., Berkman, E.A, Elmasry, N.A., Zavada, J. Luen, M.O., Reed, M.L. and Bedair, S.M. *Appl. Phys. Lett*. **86** 102504 (2005).

Ruderman, M.A. and Kittel, C. *Phys. Rev*. **96** 99 (1954).

Samant, M.G., Stohr, J., Parkin, S.S.P., Held, G.A., Hermsmeier, B.D., Herman, F., van Schilfgaarde, M., Duda, L.C., Mancini, D.C., Wassdahl, N. and Nakajima, R. *Phys. Rev. Lett*. **72** 1112 (1994).

Sanvito, S., Lambert, C.J., Jefferson, J.H. and Bratkovsky, A.M. *Phys. Rev. B* **59** 11936 (1999).

Scgrieffer, J.R. and Wolff, P.A. *Phys. Rev*. **149** 491 (1966).

Shibayama, Y., Sato, H., Enoki, T. and Endo, M. *Phys. Rev. Lett*. **84** 1744 (2000).

Sinha, B. and Ramasesha, S. *Phys. Rev. B* **48** 16410 (1993).

van Vleck, J.H. *Rev. Mod. Phys*. **25** 220 (1953).

Yamaguchi, K., Yamanaka, S. and Kitagawa, Y. Carbon-based magnetism, ed. Makarova, T. and Palacio, F.) (Elsevier 2006), p.201.

Yosida, K. *Phys. Rev*. **106** 893 (1957).

Zener, C. *Phys. Rev*. **81** 440 (1951a).

Zener, C. *Phys. Rev*. **82** 403 (1951b).

AUTHOR QUERIES

Q1. Au: Andriotis (2007) not in ref. list.
Q2. Au: 'nanographeme' – 'nanographene'?
Q3. Au: Gaussian (2003) not in ref. list.
Q4. Au: Makarova n.d. – year?
Q5. Au: McConnell (1967) not in ref. list.
Q6. Au: Schrieffer and Wolff (1966) not in Ref list.
Q7. Au: Hasegawa(1955) not in ref. list
Q8. Au: Places for all books?
Q9. Au: Androtis et al. 2007 – update?